

## In-out divertor flow asymmetries during ELMs in ASDEX Upgrade

### H-mode plasmas

M. Tsalias<sup>a\*</sup>, D. Coster<sup>b</sup>, C. Fuchs<sup>b</sup>, A. Herrmann<sup>b</sup>, A. Kallenbach<sup>b</sup>, H. W. Mueller<sup>b</sup>, J. Neuhauser<sup>b</sup>, V. Rohde<sup>b</sup>, N. Tsois<sup>a</sup> and the ASDEX Upgrade Team<sup>b</sup>

<sup>a</sup> NCSR ‘Demokritos’, Inst. of Nucl. Technology – Rad. Prot., 153 10 Ag. Paraskevi, Attica, Greece

<sup>b</sup> Max – Planck – Institut für Plasmaphysik, EURATOM Association, Garching, Germany

#### Abstract

In ASDEX Upgrade, a fast reciprocating probe positioned in the lower divertor, capable of accessing the low-field side (LFS) and high-field side (HFS) scrape-off layer (SOL) just below the x-point, as well as the private flux region, was equipped with a Mach head and used to investigate fast flow fluctuations and in-out divertor flow asymmetries during ELMs.

We compare the flow behaviour during ELMs in the three separate regions. Flow enhancement is observed in the HFS SOL, with Mach number values reaching or exceeding  $M = 2$ , flow reversal in the LFS SOL, and complex fluctuating behaviour in the private flux region (which includes flow reversal). We discuss the possible mechanisms that could drive these observations.

---

*PACS:* 52.70.-m, 52.55.Fa

*JNM keywords:* Plasma-Materials Interaction, Plasma Properties

*PSI-16 keywords:* ASDEX-Upgrade, Divertor Plasma, Divertor Diagnostic, Probes

\**Corresponding author address:* NCSR ‘Demokritos’, Inst. of Nuclear Technology – Rad. Protection, 153 10 Ag. Paraskevi, Attica, Greece

\**Corresponding author e-mail:* maximos@ipta.demokritos.gr

*Presenting author:* Maximos Tsalas

*Presenting author e-mail:* [maximos@ipta.demokritos.gr](mailto:maximos@ipta.demokritos.gr)

## **1. Introduction**

Understanding particle and power flow towards the divertor targets during ELMs is a key element for optimizing divertor operation in ITER. Although, compared with the inter-ELM phase, ELMs carry proportionally a smaller fraction of the total exhausted power [1], they are associated with large, potentially very detrimental to first wall materials, instantaneous power fluxes ([2] and references therein). In-out divertor asymmetries are a key component in this. It has been observed that ELMs typically result in an inversion of the 2:1 out/in energy deposition ratio observed in between ELMs in discharges with ion  $\mathbf{B} \times \nabla \mathbf{B}$  drift towards the active x-point [3]. When the ion  $\mathbf{B} \times \nabla \mathbf{B}$  drift is reversed however, the in/out energy deposition ratio reduces to 1:1. Since the processes behind such observations, especially the role of parallel and perpendicular particle transport, are still not completely clarified, additional observational input on this subject is crucial. Information on divertor flows during ELMs can also be important for understanding plasma exhaust and impurity migration [4].

In this paper we describe fast flow fluctuation measurements during ELMs, made with a reciprocating probe positioned in the ASDEX Upgrade lower divertor chamber, enabling accessing to both the low-field side (LFS) and the high-field side (HFS) scrape-off layer (SOL) just bellow the x-point, as well as the private flux region, thus allowing direct comparison between these three regions.

## **2. Experimental setup**

In order to minimize the power load to the probe tips (large power fluxes can result in thermal electron emission and/or arcing), a low power H-mode with type I ELMs was used with 2.5 MW NBI (AUG discharges #20343, #21414 and #21415). The probe position in the

lower divertor, the separatrix position and, for comparison, the divertor radiated power as measured by the divertor bolometer array, are shown in figure 1. Other discharge characteristics where  $\langle n_e \rangle \sim 5.2 \cdot 10^{19} \text{ m}^{-3}$  (approximately 0.5 of  $n_{GW}$ ),  $I_p \sim 800 \text{ kA}$ ,  $B_T \sim -2 \text{ T}$  (ion  $\mathbf{B} \times \nabla \mathbf{B}$  drift towards the bottom x-point),  $q_{95} \sim 3.5$  and low triangularity. In this setup, the power load to the probe is tolerable, and it can cross the divertor chamber all the way the HFS. The movement takes approximately 280 ms. The probe head consists of two graphite tips in Mach configuration (oriented in the toroidal direction), and one stand alone tip that was used to measure floating potential ( $V_{fl}$ ) fluctuations. The two Mach tips are located in the same poloidal position, and sample the flux surfaces simultaneously. The probe is equipped with a fast data acquisition system with analog bandwidth  $\sim 100 \text{ kHz}$  and sampling rate 500 kHz, providing good temporal resolution of fast fluctuations during ELMs. In order to counteract arc formation on tips during ELMs, which tend to short circuit the power supply and destroy the  $I_{sat}$  measurements, a square voltage with asymmetric up/down phases was applied to the tips. This has the advantage of “killing” during the short positive pulses ( $\sim +10 \text{ V}$  biasing of the tips) any arcs formed during the negative ( $\sim -115 \text{ V}$ ) biasing, while maximizing the time  $I_{sat}$  is measured. If such arcs are not suppressed, they typically persist for as long as the probe remains immersed in the plasma, destroying all the measurements. The disadvantage of this technique is that during the positive bias some information is lost.

### 3. The inter-ELM profile

To understand how measured flows deviate from the inter-ELM value during ELMs, it is necessary first to be aware of the measured inter-ELM profile across the probe trajectory, shown in figure 2. The ELMs were cut using the outer divertor  $H_\alpha$  signal and the measured flow is plotted only when this has returned to the pre-ELM value. The Mach numbers were calculated using the standard Hutchinson formula [5]. Concerns about this interpretation of Mach measurements are legitimate, especially in so complex a plasma environment as

described here. However, in the absence of a clearer theoretical understanding, such discussions are beyond the scope of this paper.

The characteristics of the profile shown in figure 2 can be understood as follows: Since the probe measures in the toroidal direction, positive Mach numbers indicate flow in the same direction as the toroidal field (but counter-current), and negative Mach numbers indicate co-current flow (opposing the toroidal field). The probe does not give any direct information on drifts. However, it can easily be estimated that the  $\mathbf{E} \times \mathbf{B}$  drift in the SOL (of the order of  $\sim E/B$ ) is typically an order of magnitude smaller than the parallel velocity (assuming this is of the order of  $\sim c_s$ ) and therefore the flow is predominantly oriented parallel to the magnetic field, except possibly near the poloidal field minimum in the private flux region, where the Mach number tends to zero and drift effects can therefore dominate. Elsewhere however, taking into account the local field orientation, it can be seen that in the LFS SOL and private flux regions *positive* Mach numbers indicate flow towards the divertor target plates. Conversely, in the HFS part of the private flux and in the HFS SOL, *negative* Mach numbers indicate flow towards the target plates. The positions where the probe crosses the separatrix are also indicated, as determined by the observed features of the actual  $j_{sat}^+$  measurements (see e.g. [6], [7]).

The inter-ELM profile measured by the probe is comparable to measurements in ohmic discharges (see e.g. [8]) i.e. large inter-ELM Mach numbers, of the order of  $M \sim 1.5$  are observed in the vicinity of the HFS separatrix, dropping to  $M \sim 0.5$  in the far HFS SOL. In the private flux region, the flow is relatively symmetric around the poloidal field minimum, indicating that the flow moves in the co-current direction in the HFS private flux and in the counter-current direction in the LFS private flux. Also in the private flux, the flow was found to be influenced by ELMs for longer time periods than the SOL plasma, and therefore some modulation in the private flux profile is evident even after ELMs have been cut out. In the

LFS SOL the Mach number peaks near the separatrix and near the outer vertical target with a drop in between to  $M \sim 0.3$

#### 4. Flows during ELMs

We discuss the observations starting from the HFS SOL and moving outwards to the private flux and to the LFS SOL regions.

##### 4.1 HFS SOL

An example of the flow measured in the HFS SOL during an ELM is shown in figure 3. For this measurement, the probe was positioned  $\sim 3$  cm away from the HFS separatrix. Also in this figure are given the inner and outer divertor  $H_\alpha$ , the floating potential measured by the single probe tip and the  $I_{sat}$  measurements from the upstream and downstream tips used to calculate the Mach number. During the ELM (starting at  $t \sim 3.1424$  s) the flow is transiently enhanced, reaching Mach numbers of  $\sim 2.5$ . Approximately 3 ms after the ELM, the  $I_{sat}$  measurement in both tips drops very much, the downstream one measuring almost no current. Therefore, the second maximum observed in the Mach number (around  $t \sim 3.145$  s) is probably an artifact due to the very low signal/noise ratio in the downstream pin.

In the floating potential measurement, an initial very large peak is observed as soon as the ELM occurs (at  $t \sim 3.1424$  s), lasting approximately  $\sim 0.1$  ms. A possible explanation for this peak is that it is caused by high-energy electrons ejected from the region inside the pedestal during the ELM crash [9]. Such current-carrying hot electrons are rapidly flushed from the plasma, reaching the plasma facing components faster than the bulk of the ELM plasma. When they hit the probe however, they appear as a large spike on the floating potential,  $V_{ft}$ , which, to first order, depends linearly on the local plasma electron temperature. The strong  $V_{ft}$  peak is however hardly visible in the  $I_{sat}$  measurements (only very slightly between  $t \sim 3.1424$  and  $3.1425$  s), indicating that very few of these energetic electrons can cross the probe sheath of the biased tips, and therefore the  $I_{sat}$  measurement is not greatly disturbed by them.

## 4.2 Private Flux

The sequence of ELMs measured by the probe during its outward motion in the private flux region is shown in figure 4, together with the calculated Mach numbers. A relatively complicated picture arises, due to the superposition of the ELM perturbations and the change in the inter-ELM flow measured by the probe as it moves across the private flux.

During ELMs, the flow is affected mostly in the HFS private flux, where it is observed to reverse transiently before returning to a larger value than the pre-ELM one. The relaxation to the pre-ELM value happens then relatively slowly and the Mach number value is still decreasing when the next ELM occurs.

In the LFS private flux region, the ELM is seen to also provoke a decrease and reversal of the flow, but this reversal is slightly delayed compared to the HFS. Finally, very near the LFS separatrix, the effect of the ELM on the flow is much less pronounced, and only a drop to  $M \sim 0$  is observed.

Comparing in figure 4 the ELM signature on the Mach number in the HFS and LFS private flux, it is observed that they are synchronized in their positive and negative directions, i.e. they occur approximately at the same time after each ELM is triggered. The picture that arises (summarized in figure 5) is that, contrary to the inter-ELM phase where the LFS and HFS move in opposite directions, during the ELM the plasma in the private flux moves all in the same toroidal direction. The movement is initially in the positive (counter-current) and then in the negative (co-current) direction. This can also be pictured as a movement of the private flux stagnation point, first towards the HFS and then towards the LFS. The movement is also synchronized with the HFS SOL flow. When the HFS SOL flow is enhanced, the private flux flow is positive (counter-current) and, assuming the flow remains predominantly parallel to the magnetic field lines, has an outward direction. Then, when the flow in the HFS

SOL is again reduced after the ELM, the private flux flow direction reverses.

#### 4.3 LFS SOL

Measurements in the LFS SOL are relatively difficult to perform, especially near the separatrix where the heat load associated with ELMs is very large and the probe tips tend to arc/emit. Some measurements have been made, however, but relatively far from the separatrix. An example is given in figure 6, where the calculated Mach number and the associated ELM  $H_\alpha$  signal are shown, measured by the probe positioned approximately 6 cm away from the separatrix. Immediately after the ELM, the flow is seen to reverse. Even at this distance from the separatrix, however, there are many uncertainties relating to these measurements, concerning mainly the accuracy of  $I_{sat}$  measurements and whether they are seriously corrupted by factors such as the probe collection length (which very near the LFS target plates can be comparable to the connection length), by electron emission from the tips due to overheating, by fast thermoelectric electrons crossing the probe sheath or even by non-saturation of the tips due to the extremely high temperature of the plasma ejected by the ELM (the pedestal electron temperature for these shots was  $\sim 400$  eV and if plasma with a relatively large fraction of this temperature reached the probe position the error could be significant).

### 5. Conclusions and discussion

Flow fluctuations were measured in the ASDEX Upgrade divertor during ELMs. Transient flow enhancement was observed in the HFS SOL, while in the LFS the flow was seen to reverse direction and (assuming the main component of the flow is along the field lines and drifts to do not locally dominate the flow direction) move transiently away from the target plates. Such backflow has already been demonstrated numerically in the LFS SOL using B2-Eirene for the AUG Div I divertor [10]. The key mechanism driving the reversal was identified as the increased plasma pressure in front of the target plates due to enhanced recycling during ELMs.

However, it is also possible that the SOL flow could be strongly affected by momentum input from the main plasma, disturbing the outer SOL stagnation point position, located in the inter-ELM phase between the LFS mid-plane and divertor target [11]. Indeed, there is evidence suggesting that other mechanisms in addition to the “enhanced local pressure due to recycling” could be at work. For example, measurements with the probe made in upper single-null discharges at ASDEX Upgrade (the probe crosses the 2<sup>nd</sup> separatrix above the 2<sup>nd</sup> x-point, corresponding to the top SOL in lower single-null) have shown that the SOL flow can be strongly reduced during ELMs even very far from the target plates.

In JT-60U, where similar measurements as the ones presented here were performed [12], the flow was observed to reverse in the HFS SOL, i.e. contrary to what was measured here. In that case, the probe sampled the plasma higher up in the SOL, and possibly the measurement is affected by the position of the probe, i.e. whether it is located inside or above the recycling region. Indeed, if enhanced recycling was the dominant mechanism, it can be argued that upstream flow reversal might be observed above the recycling region both in the LFS and HFS. This suggests a different explanation, one that involves the global SOL flow structure.

In the private flux region, the situation is even more complicated and the observed reversal could be explained by a number of other mechanisms, such as dominant  $\mathbf{ExB}$  drifts in the vicinity of the stagnation point or by the in/out divertor pressure asymmetry which could change during ELMs. Further modeling in the Div IIb divertor geometry (including drifts) is required to clarify this point.



## References

- [1] Fundamenski W. et. al., Nucl. Fusion 45 (2005) 950.
- [2] Loarte A. et. al., Plasma Phys. Contr. Fusion 45 (2003) 1549.
- [3] Eich T., these proceedings.
- [4] Pitts R. A. et. al., Plasma Phys. Contr. Fusion 47 (2005) B303.
- [5] Hutchinson I. H., Phys. Fluids B, 3 (1991) 847.
- [6] Tsois N. et. al. Europhys. Conf. Abstr. 11D (1984) 658.
- [7] Tsalas M. et. al., J. Nucl. Mater., 337 (2005) 751.
- [8] Tsalas M. et. al., Plasma Phys. Contr. Fus., submitted.
- [9] Bergmann A., Nucl. Fusion 42 (2002) 1162
- [10] Schneider R. et. al., 16th IAEA Conference on Fusion Energy (1996) 465.
- [11] Mueller H.W. et. al., these proceedings.
- [12] Asakura N. et. al., Plasma Phys. Contr. F. 44 (2002) A313.

## List of Figures

Fig.1. Position of the reciprocating arm at full extension wrt. the magnetic separatrix for the discharge discussed in this paper (# 21414). Also shown is the tomographic reconstruction of the radiated power, as measured by the AUG divertor bolometer array.

Fig.2. Inter-ELM Mach number profile across the probe trajectory in discharge # 21414.

Fig. 3. HFS measurements. From top to bottom: a) inner (red) and outer (blue) divertor  $H_{\alpha}$ , b) floating potential measured by the probe single tip, c) current measured by the Mach probe upstream (red) and downstream (black) tips and d) calculated Mach number.

Fig. 4. From top to bottom: a) inner (red) and outer (blue) divertor  $H_{\alpha}$ , b) floating potential measured by the probe single tip and c) calculated Mach number during the probe outward crossing of the private flux region.

Fig. 5. An overview of the observed HFS SOL and private flux flows during an ELM. The blue and red arrows indicate the toroidal flow direction measured by the probe. Blue indicates flow towards and red flow away from the target plates. The green arrows indicate the inferred poloidal flow.

Fig. 6. LFS measurements: From top to bottom: a) inner (red) and outer (blue) divertor  $H_{\alpha}$  and b) calculated Mach number.

Figure 1

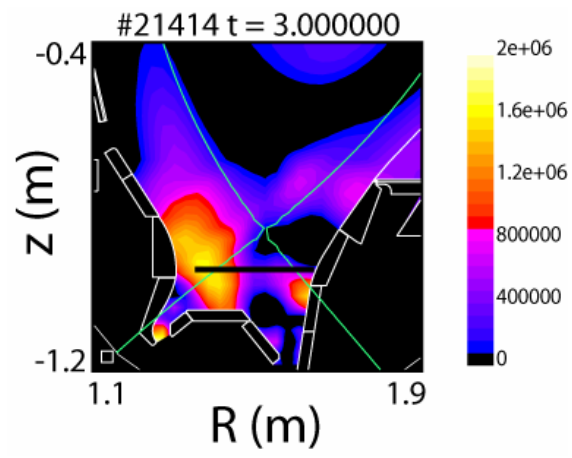


Figure 2

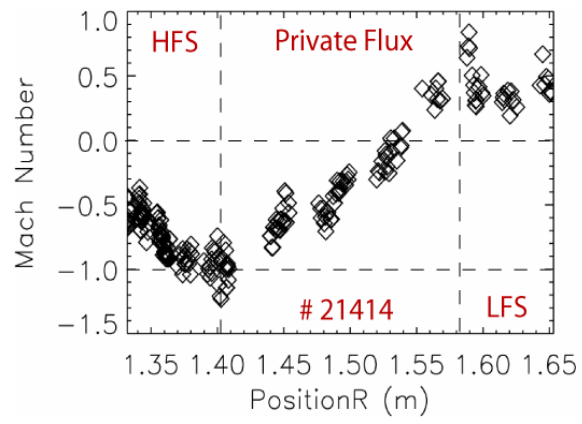


Figure 3

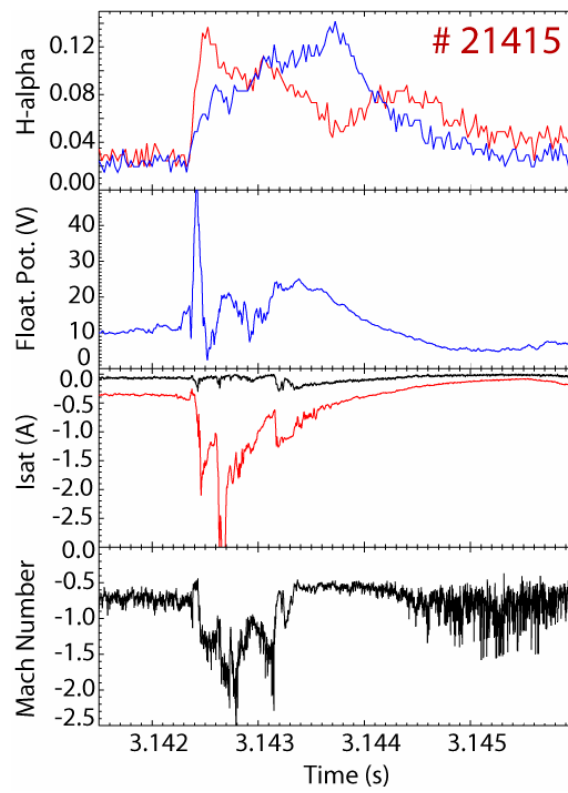


Figure 4

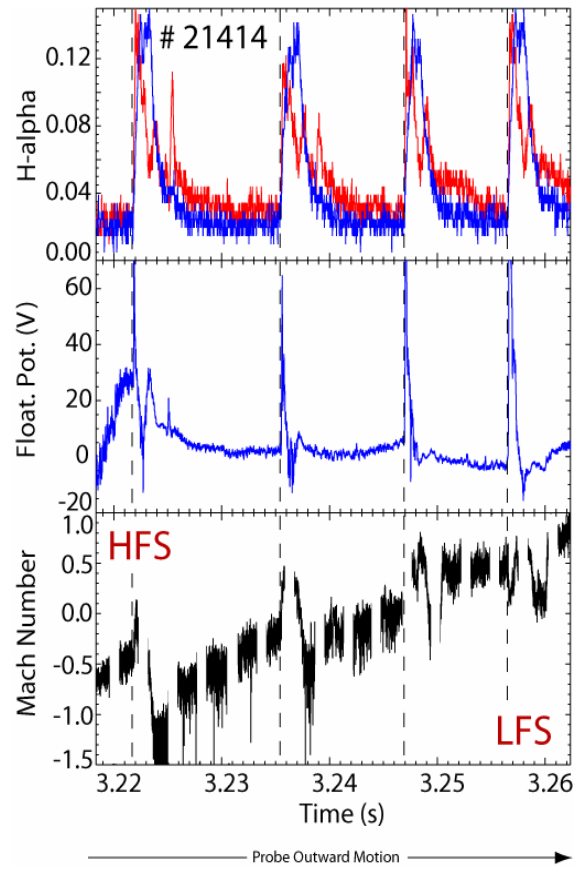


Figure 5

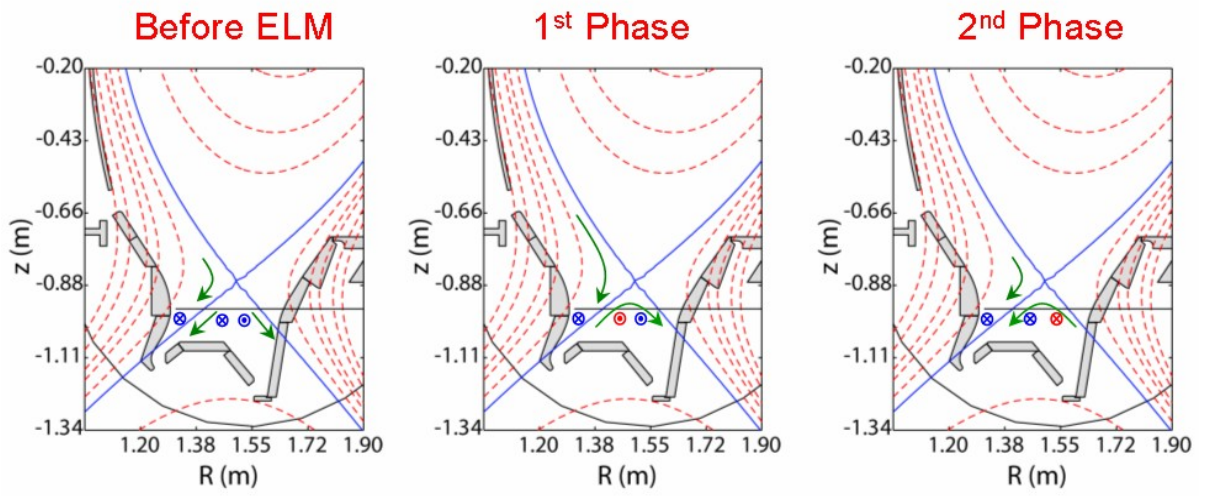


Figure 6

